Energy Conversion and Management: X 27 (2025) 101163

Contents lists available at ScienceDirect

Energy Conversion and Management: X

journal homepage: www.sciencedirect.com/journal/energy-conversion-and-management-x

Role of wind speed and solar irradiation on the cost of medium-sized off-grid hybrid renewable energy systems under challenging weather conditions

MohammadReza Akhtari *, Oskar Karlström

Industrial Engineering and Management, Department of Mechanical and Materials Engineering, University of Turku, Turun Yliopisto, 20014 Turku, Finland

ARTICLE INFO

Keywords:
Hybrid renewable energy
HRES
Nordics
Wind energy
Solar energy
Techno-economic assessment

ABSTRACT

The present study investigates the role of wind speed and solar irradiation on the cost of medium-sized energy systems under weather conditions characterised by long winters and summers with extended sunlight hours. The study models and optimises different configurations of off-grid hybrid energy systems for 100 persons for conditions of 20 different cities, using hourly input data of solar irradiation, ambient temperature, and wind speed. In total, more than 500,000 data points are used in the multi-variable optimisation. In these cities, the average (throughout the year) wind speed varies between 2.32 and 7.23 m/s, and the solar irradiation varies from 1.94 to 3.61 kWh/m^2/day. The winters for the investigated cities are long (several months), with solar irradiation less than 0.5 kWh/m^2/day. The optimised systems consist of small-scale wind energy, solar energy, batteries, and biodiesel generators as backup energy. For the optimised systems with wind energy, the results show that the levelized costs range between 0.16 and 0.48 $/kWh. For the optimised systems without wind energy, the cost ranges from 0.44 to 0.63 $/kWh. These results give new insight into when additional energy sources may be needed in medium-sized energy systems. Finally, a sensitivity analysis shows that even small-scale off-grid systems without wind energy may soon be a viable option for reaching competitive energy prices with existing technologies.

Introduction

Globally, 46 % of power capacity installation is today related to renewable energy [1], although fossil fuels (coal, natural gas, and oil) still account for around 80 percent of the world's primary energy consumption. The Nordic countries (Finland, Sweden, Norway, Denmark, Iceland, and the Faroe Islands) have high ambitions to reach carbon neutrality [2,3]. The electricity production methods vary among the Nordic region and are mostly based on renewable energy resources. The highest shares of electricity generation methods were 54 % with wind energy in Denmark, 35.1 % with nuclear energy in Finland, 88.1 % with hydro energy in Norway, 40.6 % with hydropower in Iceland, 40.6 % with hydro energy in Sweden in 2022, and around 47.8 % of electricity demand based on wind energy in the Faroe Islands in 2023 [4,5]. The high use of wind energy in these countries today would not be possible without the presence of hydropower, supporting the electricity supply during wind-free days. The electricity market in Denmark, Sweden, and Norway is based on small zonal prices (five zones in Norway, four in Sweden, two in Denmark, and one in Finland), influencing the flexibility and system costs for energy transition [6,7]. This part of the world enjoys long, bright summer days with 20 to 30 times higher solar energy than in the wintertime, which could be utilised to satisfy electricity and heating demand when it is combined with appropriate energy storage units, especially at more cost-effective prices on larger scales [8,9]. However, solar energy in this area has become less common than in other parts of Europe, partly explained by less sun during the winter [10]. Furthermore, the Nordic regions take advantage of abundant wind energy with a newly installed capacity of nearly 5 GW in 2024 and a cumulative amount of almost 40 GW [11].

Despite the European Climate Law to attain climate neutrality in the long term by 2050 [12], Nordic countries have a high ambition of achieving this target by 2030 in Norway, by 2035 in Finland, by 2040 in Iceland, by 2045 in Sweden and by 2050 in Denmark [13]. This is while the Nordics face harsh climatic conditions with low solar radiation and high-energy-demanding industries [14]. Nordics, as a pioneer in clean energy and net-zero emissions achievement, has developed various projects to facilitate this pathway, such as Nordic hydrogen valleys as

* Corresponding author.
E-mail address: mohammadreza.akhtari@utu.fi (M. Akhtari).

https://doi.org/10.1016/j.ecmx.2025.101163
Received 22 May 2025; Received in revised form 20 July 2025; Accepted 21 July 2025
Available online 23 July 2025

Nomenclature

Abbreviations

AC	Alternative current
BT	Battery
CAPEX	Capital expenditure
CC	Cycle charging
DC	Direct current
DG	Diesel generator
DOD	Depth of discharge
EU	European Union
Fingrid	Finland's transmission system operator
HOMER	Hybrid optimisation of multiple energy resources
HRES	Hybrid renewable energy systems
LCOE	Levelized component cost of energy
LF	Load following
NOCT	Nominal operating cell temperature
NPC	Net present cost
OPEX	Operating expense
PV	Photovoltaics
SOC	State of charge
WT	Wind turbines

Parameters

A_i	Anisotropy index
B (0.00650 K/m)	Lapse rate
$C_{annualised}$ ($)	Annualised component cost
c	Storage capacity ratio
f_d (%)	Derating factor
g (9.81 m/s^2)	Gravitational acceleration
$\overline{G}_b$ (k W/m^2)	Beam radiation
$\overline{G}_d$ (k W/m^2)	Diffuse radiation
$G_{(T,STD)}$ (1000 W/m^2)	Incident radiation at standard conditions
G_T (W/m^2)	Actual global solar radiation incident
G_{NOCT} (0.8 kW/m^2)	Solar irradiation at NOCT
h_{hub} (m)	Wind turbine hub height
I_{max} (A)	Maximum charging current
N	Number of each component
n (year)	Project lifetime
$P_{(cmax,KiBaM)}$ (W)	Maximum capacity based on the Kinetic battery model
$P_{(cmax,MCC)}$ (W)	Maximum charge power based on the maximum charging current
$P_{(cmax,MCR)}$ (W)	Maximum capacity based on the maximum charging rate
$P_{(dmax,KiBaM)}$ (W)	Maximum discharging power
$P_{(WT,STP)}$ (W)	Wind turbine power output
P_{pv} (W)	PV energy output
P_{rt} (W)	PV output at the standard conditions
P_{WT} (W)	Actual WT-generated power
Q_{max} (kWh)	Maximum capacity of the battery
R (287 J/kg/K)	Gas constant
r (%)	Real discount rate
T (K)	Actual temperature
T_0 (288.16 K)	Standard temperature
U_{hub} (m/s)	Wind speed at the hub height
U_{ref} (m/s)	Wind speed at the reference point
V_{nom} (V)	Nominal voltage of the battery
z (m)	Altitude
Z_0 (m)	Surface roughness length

Greek symbols

α_c (A/(Ah))	Battery maximum charge rate
α_t (%/°C)	Power temperature coefficient
β (°)	Surface slope
$\eta_{mp,STD}$ (%)	Maximum power efficiency under standard conditions
$\eta_{cbattery}$ (%)	Battery charge efficiency
$\eta_{dbattery}$ (%)	Battery discharge efficiency
η_{inv} (%)	Inverter efficiency
η_{rect} (%)	Rectifier efficiency
$\eta_{roundtrip}$ (%)	Round-trip battery efficiency
$\theta_{\alpha,NOCT}$ (20 °C)	Ambient temperature at NOCT
θ_c (°C)	Actual temperature
θ_{STD} (25 °C)	Standard temperature
θ_z (o)	Zenith angle
ρ (kg/m^3)	Ambient density
ρ_g (%)	Ground reflection (albedo)
ρ_0 (kg/m^3)	Air density at the standard condition

energy hubs, the clean energy transition partnership, the Nordic energy research mobility, Nordic energy systems, Nordic maritime transport and energy research, bioenergy value chain programs, green transition initiative, and so on [15]. Policies and regulations have been updated over time by various countries and the European Union, such as the carbon border adjustment mechanism [16], European green deal, Environment action program to 2030, REPowerEU, Clean industrial deal, Fit for 55, EU emissions trading system, and net-zero industry act to accelerate this transition by adopting clean energy sources while steadily eliminating fossil fuels to satisfy the minimum 55 % decrease in greenhouse gas emissions as the intermediate goal by 2030, compared to its value in 1990 [17,18].

Wind and solar energy play a crucial role in the green energy transition. The high amount of variable wind energy necessitates balancing power at various time scales, such as different storage systems or other resources coupling to overcome the mismatch between supply and demand, as the wind energy follows quite the same pattern in this region and the uncertainty in forecasting [19,20]. One study in Nordic conditions showed that integrating wind energy into solar energy systems could reduce the life cycle cost by as much as 32 % [21]. Norway installed the most onshore wind energy capacity in 2020, while Sweden achieved the first position in 2021 in Europe and together with Finland in 2022 in the Nordic region [22]. It was shown that small wind turbines can generate more power than PV annually in Poland; however, large-scale wind turbines generate electricity at a lower price, thanks to the economies of scale. Today, with capacity factors as low as 20 %, small-scale wind turbines can be cost-competitive [23]. Despite various studies on wind energy and techno-economic assessment, there is still a need for further and in-depth investigation in specific contexts [24]. Although solar panels receive a larger amount of reflected irradiation as a result of the albedo effect in snow-covered surroundings and achieve better efficiency at lower temperatures, the soiling impact, together with the dark winter days and rapid weather changes, could impose a major issue during the wintertime. Cloudy and snowy days also influence the mismatch between supply and demand [25]. It has, however, been shown that it is possible to supply the whole energy demand of buildings under the Nordic climatic conditions to achieve a net-zero or even positive energy building by having better energy-efficient buildings. Further, this energy supply should be integrated with harvesting or importing additional renewable energy, such as taking advantage of wind turbines, which also leads to the supply and demand matching improvement, as well as more photovoltaic thermal panels than what is available on rooftops in buildings [26].

To further accelerate renewable energy adoption, several different strategies could be used. One alternative could be to incentivise the implementation of hybrid renewable energy systems (HRESs). Off-grid

HRES could support energy supply in remote areas, but also offers more stable energy prices. Further, partly or fully relying on HRES also provides de-risking from a cybersecurity point of view. However, research is scarce on the specific role of wind speed and solar irradiation on the cost of HRES under challenging weather conditions, such as those in the Nordic countries. The price of green technologies has experienced a significant decrease over the past few years (35 % in solar panels and 54 % in lithium iron phosphate in 2024 [27]). It is also supposed to reduce up to 11 % in 2025 and its levelized cost of electricity up to almost 50 % by 2035 [28], which requires updated research in this field. The energy technology prices have reduced dramatically, as well as the feasibility and configurations of HRES have changed, which motivates the optimisation and modelling of new systems.

The present study investigates the role of wind speed and solar irradiation on the cost of medium-sized energy systems under weather conditions characterised by long winters and summers with extended sunlight hours. The study models and optimises off-grid hybrid energy systems for 100 persons for conditions of 20 different cities in Nordic countries, using hourly input data of solar irradiation, ambient temperature, and wind speed (in total, more than 500,000 data points are used in the optimisation). To our knowledge, these kinds of results have not been demonstrated earlier for such challenging weather conditions. In these cities, the average (throughout the year) wind speed varies between 4.5 and 9.8 m/s, and the solar irradiation varies from 2.1 to 3.1 kWh/m^2/day. The winters for the investigated cities are long (several months), with solar irradiation less than 0.5 kWh/m^2/day.

Methodology

Following the previous works to address the earth-air heat exchanger [29] and hydrogen integration [30] into the HRES, here, a hybrid renewable energy system, comprising wind turbines (WT), solar panels or photovoltaics (PV), chemical battery energy storage (BT), inverter, and backup biodiesel generator as a supportive supply, is studied in 20 cities of Northern Europe in the direction of obtaining the most cost-effective energy supply configuration based on the techno-economic assessment. The analysis is performed based on the hourly data and optimisation in HOMER [31], which has been validated and discussed in the earlier study [32].

Various simulation software has been used to simulate and optimise energy systems such as HYBRID2, HOMER, RETScreen, iHOGA, TRNSYS, INSEL, SOLSIM37, and ARES [33,34], among which HOMER (Hybrid Optimisation Model for Multiple Energy Resources) is extensively used to investigate HRESs with the appropriate database and flexibility [35]. This software is appropriate for HRES sizing, which is provided by the National Renewable Energy Laboratory (NREL) and optimises the NPC based on the hourly assessment. However, various tools could be integrated and used together to enhance the capabilities and functionalities [36]. HOMER Pro also provides detailed results with vigorous simulation and modelling, although modelling details remain to be discovered [37].

For each city, the hourly data of solar irradiation, wind speed and temperature are used together with hourly electricity consumption data. In order to enable a sounder comparison of the different systems, the electricity consumption is assumed to be the same as the average consumption in Finland in 2023. It should be noted that in every city (even in the same country), the average electricity consumption differs.

The cities are located in the five Nordic countries (Finland, Sweden, Norway, Denmark, and Iceland). The graphical overview of the considered HRES is illustrated in Fig. 1, where wind turbines and a biodiesel generator produce an alternating current (AC), and electrical demand requires AC, while solar panels and a chemical battery operate in direct current (DC).

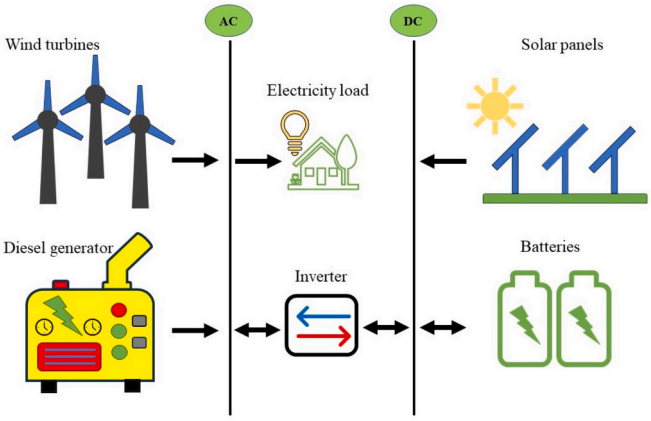

Fig. 1. Components of the investigated energy system (HRES).

Wind energy

Wind energy constituted 8.1 % of electricity generation worldwide in 2024 [38]. The wind turbine output is affected by the wind speed and power curve, which is exclusive for each wind turbine, showing the wind turbine's power output at a working range of wind speed. The wind turbine usually starts working at a certain wind speed called the cut-in speed. Then, its power output reaches the maximum amount called rated power at rated speed until it stops working again at cut-out speed due to safety. It is worth mentioning that the measured wind speed of $U_{ref}(m/s)$ varies at different heights, and it is important to calculate the wind speed of $U_{hub}(m/s)$ at the hub height of $h_{hub}(m)$, which is influenced by the surface roughness length of $Z_0(m)$ [39].

$$U_{hub} = U_{ref} * H(h_{hub}) \tag{1}$$

$$H(h_{hub}) = \frac{ln(h_{hub}/Z_0)}{ln(h_{ref}/Z_0)} \tag{2}$$

Although the wind turbine's power output of $P_{WT,STP}(\mathrm{W})$ in the standard condition is obtained through the power curve provided by the manufacturer, the actual generated power of $P_{WT}(\mathrm{W})$ is scaled in terms of the relationship between the standard, $\rho_0(\mathrm{kg/m^3})$, and ambient density, $\rho(\mathrm{kg/m^3})$ [40].

$$P_{WT} = \left(\frac{\rho}{\rho_0}\right) P_{WT,STP} \tag{3}$$

Assuming the linear temperature relationship, $T = T_0 - Bz$, as well as considering the ideal gas formula, $\rho = P/(RT)$, the ratio of air density can be obtained and the ratio of densities can be adjusted at the hub height based on the standard temperature, $T_0(288.16\mathrm{K})$, lapse rate, $B(0.00650\mathrm{K/m})$, gas constant, $R(287\mathrm{J/kg/K})$, gravitational acceleration, $g(9.81\mathrm{m/s^2})$, and altitude, $z(m)$.

$$\frac{\rho}{\rho_0} = \frac{P}{P_0}\frac{T_0}{T} \tag{4}$$

$$P = P_0\left(1 - \frac{Bz}{T_0}\right)^{\left(\frac{g}{RB}\right)} \tag{5}$$

$$\frac{\rho}{\rho_0} = \left(1 - \frac{Bz}{T_0}\right)^{\frac{g}{RB}}\left(\frac{T_0}{T_0 - Bz}\right) \tag{6}$$

Various wind turbines have been tried to select the one that delivers electricity at a low price. EO10 is a small wind turbine made by Eocycle that can be used in residential buildings and small communities, and reaches the rated power at a wind speed of 6.5 m/s (Table 1).

Table 1
Wind turbine technical and economic details.

Wind turbine	
Type	Horizontal
Nominal capacity	10 kW
Rated wind speed	6.5 m/s
Hub height	16 m
Number of blades	3
Rotor diameter	15.81 m
Cut-in wind speed	2.75 m/s
Cut-out wind speed	20 m/s
Survival wind speed	52.5 m/s
Lifetime	20 years
Capital cost	2000 $/kW
Replacement cost	1800 $/kW
O&M cost	30 $/unit/year

Table 2
PV techno-economic properties.

Solar panel	
Type	Flat plate
Model	CS6X-325P
Manufacturer	Canadian Solar
Technology	Polycrystalline
Rated capacity	0.325 kW
Derating factor	88 %
Efficiency	16.94 %
Nominal operation cell temperature	45 °C
Temperature coefficient	−0.41 %/°C
Lifetime	25 years
Capital cost	950 $/kW
Replacement cost	900 $/kW
O&M cost	10 $/kW/year

Solar photovoltaics (PV)

Solar energy is responsible for 6.9 % of the global electricity generation mix in 2024 [38]. Taking advantage of solar PV, temperature inversely affects a solar panel's efficiency and the produced energy, P_{pv}(W), which is a function of a derating factor, f_d(%), standard temperature, θ_{STD} (25 °C), power temperature coefficient, α_t (%/°C), incident radiation at the standard condition, $G_{T,STD}(1000\text{W/m}^2)$, actual global solar radiation incident, $G_T(W/m^2)$, actual temperature, θ_c (°C), and PV output at the standard condition, $P_{rt}(W)$ [41,42].

$$P_{pv} = P_{rt} f_d \left(\frac{G_T}{G_{T,STD}}\right)(1 + \alpha_t(\theta_c - \theta_{STD}))\tag{7}$$

The cell temperature in Kelvin is calculated at each time step as:

$$\theta_c = \frac{\theta_a + (\theta_{c,NOCT} - \theta_{a,NOCT})\left(\frac{G_T}{G_{T,Noct}}\right)\left(1 - \frac{\eta_{mp,STD}(1-\alpha_t\theta_{STC})}{\tau\alpha}\right)}{1 + (\theta_{c,NOCT} - \theta_{a,NOCT})\left(\frac{G_T}{G_{T,NOCT}}\right)\left(\frac{\alpha_t\eta_{mp,STD}}{\tau\alpha}\right)}\tag{8}$$

where, $\eta_{mp,STD}$(%) is the maximum efficiency point of power at the standard condition, τ(%) is solar transmittance, α(%) is the PV solar absorptance, $\theta_{c,NOCT}$ (°C) is the nominal operating cell temperature (NOCT), $G_{T,NOCT}(0.8\text{kW/m}^2)$ is the solar radiation at NOCT, and $\theta_{a,NOCT}$ (20 °C) is the ambient temperature at NOCT. The value of $\tau\alpha$ is proposed to be 0.9 by Duffie and Beckman [43].

The global horizontal irradiance (GHI), which is the total amount of radiation from the sun on the horizontal plate on the earth, is used at each time step to compute the PV power output. However, the PV surface is usually tilted, and the solar irradiation should be recalculated as below.

$$\overline{G}_T = (\overline{G}_b + \overline{G}_d A_i)R_b + \overline{G}_d(1 - A_i)\left(\frac{1 + cos(\beta)}{2}\right)\left(1 + fsin^3\left(\frac{\beta}{2}\right)\right) + \overline{G}\rho_g\left(\frac{1 - cos(\beta)}{2}\right)\tag{9}$$

Here, the surface slope is $\beta(^\circ)$, albedo or reflection from the ground is ρ_g(%), the beam radiation is $\overline{G}_b(\text{kW/m}^2)$, the diffuse radiation is $\overline{G}_d(\text{kW/m}^2)$, the time-step average of GHI is $\overline{G}(\text{kW/m}^2)$, the anisotropy index or the atmospheric beam radiation transmittance is $A_i(=\overline{G}_b/\overline{G}_0)$, and the beam ratio on the tilted and horizontal surface is $R_b(=\cos\theta/\cos\theta_z)$, where the zenith angle is $\theta_z(^\circ)$ and the time-step average of extra-terrestrial horizontal radiation $\overline{G}_0(\text{kW/m}^2)$.

Table 2 demonstrates the technical and economic properties of solar panels in the energy system. As can be seen, the temperature has an inverse effect on the PV efficiency. Moreover, it experiences less degradation in Nordic countries due to the colder weather conditions compared to the lower latitudes.

Biodiesel generator and converter

The converter consists of an inverter and rectifier, which can convert current between AC and DC. The output power scales with the efficiency of the inverter, η_{inv}(%), and rectifier, η_{rect}(%), and with more detail in Table 3.

Regarding a biodiesel generator and due to the intermittency of renewables, the generator should be able to cover the whole demand independently. Therefore, a diesel generator, also functioning for biodiesel, of 150 *kW* (Table 4) is selected in order to meet a 10 % higher load as safety than the peak demand, which is equal to 136.07 kW. Table 5 demonstrates the effect of generator size on the energy deficit in Trondheim, with the highest amount of biodiesel requirement. The 10 % larger generator could solely meet the electrical demand without any energy shortage, which is an important parameter for the stand-alone system. A 10 % higher capacity constraint is considered to overcome the fluctuation in energy demand.

Energy storage

A storage unit has been shown with various applications and benefits in the literature. Appropriate battery storage contributes to generating less emissions, lowering the electricity price and oscillations, facilitating grid connection, shifting loads, and improving energy security. Renewable energy is inherently intermittent and is essential to be integrated with other sources of energy or storage systems to constantly balance supply and demand. Covering the peak demand could be significantly expensive, and batteries are possible to be used to shave the peak demand and avoid costly oversized systems. Dispatch strategy identifies the energy stream, here, the electricity movement between various components in the energy system. Here, the study considers two dispatch methods for battery charging, namely load following, where only a primary load is met by a biodiesel generator, and cycle charging, where all demands and batteries are supplied by a biodiesel generator [44]. At each step, the available energy, as well as demand and loss, are calculated to decide whether to charge or discharge the storage units if any surplus electricity is available ($E_{charge,discharge} \geq 0$).

$$E_{available} = E_{pv} + E_{wind} + E_{net}\tag{10}$$

Table 3
Converter data of HRES.

Converter	
Rectifier efficiency	95 %
Inverter efficiency	95 %
Rectifier capacity	100 %
Lifetime	15 years
Capital cost	171 $/kW
Replacement cost	171 $/kW
O&M cost	4 $/kW/year

Table 4
Biodiesel generator details in the study.

Diesel generator	
Capacity	150 kW
Consumption	0.25 l/h/kW
Biodiesel price	2 $/l
Lifetime	90,000 h
Capital cost	175 $/kW
Replacement cost	175 $/kW
O&M cost	0.1 $/h

Table 5
Biodiesel generator study and effect on the optimal system in Trondheim, Norway.

DG (kW)	LCOE ($/kWh)	Diesel (L)	Capacity shortage (kWh/year)
137	0.478462	41,756	52.8
143	0.481538	51,951	13.3
150	0.484615	42,823	0
157	0.489231	42,781	0
165	0.489231	47,505	0

$$E_{consumption} = E_{load} + E_{loss,converter} + E_{loss,battery} \tag{11}$$

$$E_{charge,discharge} = E_{available} - E_{consumption} \tag{12}$$

Finally, the maximum charging power is limited by three criteria, namely maximum charging current ($P_{cmax,MCC}$), maximum charging rate ($P_{cmax,MCR}$), and maximum capacity based on the kinetic battery model ($P_{cmax,KiBaM}$) as the storage unit cannot collect all the available energy in the system [45,46].

$$P_{cmax,MCC} = \frac{N_{bat} I_{max} V_{nom}}{1000} \tag{13}$$

$$P_{cmax,KiBaM} = \frac{-kcQ_{max} + kQ_1 e^{-k\Delta t} + Qkc\left(1 - e^{-k\Delta t}\right)}{1 - e^{-k\Delta t} + c(k\Delta t - 1 + e^{-k\Delta t})} \tag{14}$$

$$P_{cmax,MCR} = \frac{(1 - e^{-a_c \Delta t})(Q_{max} - Q)}{\Delta t} \tag{15}$$

$$P_{cmax} = \frac{Min\left(P_{cmax,KiBaM}, P_{cmax,MCR}, P_{cmax,MCC}\right)}{\eta_{cbattery}} \tag{16}$$

The kinetic battery model is also used to compute the maximum discharge power ($P_{dmax,KiBaM}$), indicating the ultimate amount that energy could be delivered on an hourly basis considering the discharge energy loss of η_d [47].

$$P_{dmax,KiBaM} = \frac{kQ_1 e^{-k\Delta t} + Qkc\left(1 - e^{-k\Delta t}\right)}{1 - e^{-k\Delta t} + c(k\Delta t - 1 + e^{-k\Delta t})} \eta_{dbattery} \tag{17}$$

Then, the state of charge (SOC) can be calculated after each discharge or charge cycle as:

$$SOC = \frac{E_{battery,after}}{N_{battery} V_{nom} Q_{max}} \tag{18}$$

SOC(t) at each time step is constrained between the maximum and minimum amount, with the latter one being computable through the percentage of depth of discharge (DOD) [48].

$$\mathrm{SOC}_{min} \leq \mathrm{SOC(t)} \leq \mathrm{SOC}_{max} \tag{19}$$

$$SOC_{min} = 1 - DOD \tag{20}$$

Here, the battery energy before charge or discharge, the minimum available energy, and the net available energy in the batteries are obtained based on:

$$E_{battery} = N_{battery} V_{nom} Q_{max} \tag{21}$$

$$E_{min} = E_{battery} SOC_{min} \tag{22}$$

$$\eta_{battery} = \sqrt{\eta_{roundtrip}} \tag{23}$$

$$E_{net} = \left(E_{battery} - E_{min}\right)\eta_{battery} \tag{24}$$

where, $Q_{max}(kWh)$ is the maximum battery capacity, $k\left(h^{-1}\right)$ is the storage rate constant, $\Delta t(h)$ is the time step length, c is the storage capacity ratio, $Q_1(kWh)$ is the available battery energy at the start of the time step, $Q(kWh)$ is the total battery energy at the start of the time step, $\eta_{roundtrip}$ is the round-trip efficiency of the battery, $a_c(A/(Ah))$ is the maximum charge rate of the battery, $N_{battery}$ is the number of batteries, $V_{nom}(V)$ is the nominal voltage of the battery, $I_{max}(A)$ is the maximum charge current of the battery, $\eta_{cbattery}$ and $\eta_{dbattery}$ are the charge and discharge efficiency of the battery, respectively. The techno-economic specifications of the considered chemical batteries are mentioned in Table 6.

Rationale behind technology selection

The Canadian Solar CS6X-325P panel has a power tolerance of almost 5 W, which has durability in corrosive surroundings. It is suitable for not only residential but also industrial installations on the rooftop or as a ground-mounted system with a 25-year performance warranty for linear energy generation. Furthermore, it is appropriate in Nordics due to its acceptable functionality at a low amount of irradiance, with more than 95 % performance and could bear a high amount of load, such as snow [49]. Considering wind energy, various wind turbines have been tested to see which one leads to the highest power generation under the considered climatic conditions. Eocycle EO10 also has a large operating range with the cut-in and cut-out wind speeds of 2.75 and 20 m/s respectively, which is suitable for the Nordic regions, where wind speed varies significantly. Furthermore, the small wind turbine could be used in more local and residential places with the scalability possibilities.

Lithium-ion storage battery, where the cathode is made of lithium metal oxide, has a fast response time, low maintenance, environmental advantage, durability to heat, high energy density and round-trip efficiency, with a consistent power output and without a memory effect [50,51]. Li-ion battery has a long cycle life, reliability and calendar life but lower storage depletion, self-discharge rate, and loss compared to a lead-acid battery [52,53]. A biodiesel generator, as mentioned earlier, is selected to be able to deliver 10 % more energy than the peak demand without any energy shortage, considering also 10 % reserved capacity

Table 6
Battery techno-economic specification.

Storage battery	
Manufacturer	Saft
Technology	Lithium-ion
Nominal capacity	55 kWh
Nominal voltage	720 V
Round-trip efficiency	97 %
Max charge current	82 A
Max discharge current	200 A
Initial charge	100 %
Capacity ration	0.927
Lifetime throughput	240 MWh
Lifetime	20 years
Maximum charge rate	1 A/Ah
Optimal depth of discharge	90 %
Cycle life (80 % DOD at 25 °C)	5250 cycles
Capital cost	180 $/kWh
Replacement cost	180 $/kWh
O&M cost	150 $/year

for unpredictable fluctuations in energy demand. It is important to have a backup due to the intermittency of renewables and to increase the safety of HRES. It also helps to avoid oversizing and reduce the cost of the system in some cases, while it could pose an environmental burden in other cases, such as Norway, where more than 40 % of total energy and almost 90 % of electricity generation comes from hydropower [54].

Climatic condition

The hourly solar irradiation, wind speed, and ambient temperature for the investigated cities are obtained, and their annual average is summarised in Table 7. The highest average annual solar radiation, wind speed, and temperature are those of Copenhagen, Tórshavn, and Aarhus. On the other hand, the lowest amounts are those of Tórshavn, Trondheim, and Nuuk, respectively. The climatic data at high resolution in 2023 are extracted from the Finnish Meteorological Institute [55], Danish Meteorological Institute [56], Norwegian Centre for Climate Services [57], Photovoltaic Geographical Information System [58], Icelandic Meteorological Office [59], and NASA POWER [60].

Electrical load

Taking the electricity consumption data in Finland provided by Fingrid (Finland's transmission system operator) [61] into account, the average hourly electricity consumption for 100 Finnish individuals is calculated based on the total electricity consumption, where the industrial electricity is subtracted. Fig. 2 demonstrates the average hourly electricity consumption of 100 Finnish individuals in 2022. The annual electricity consumption is 782 *MWh* as an alternating current. The minimum electricity demand occurs in July, while the highest amount takes place in January.

Economic parameters

The most optimum system is ranked on the basis of the objective function, which is equal to the net present cost (NPC) [62]. Then, NPC is used to compute the levelized component cost of energy (LCOE), which is the electricity price per unit of consumed or served electricity. Here, LCOE ($/*kWh*) gives the cost of energy, considering the price of all the annualised components, which excludes other costs such as

Table 7
The annual average of solar irradiation, wind speed, and temperature for 20 cities in 2023.

Region	Cities	Irradiation (kWh/m^2/day)	Wind speed (m/s)	Temperature (°C)
Finland	Turku	2.98	3.29	6.09
	Helsinki	2.90	4.25	6.95
	Oulu	2.63	4.88	3.56
	Tampere	2.30	3.26	5.29
Åland Islands	Mariehamn	3.04	3.98	6.78
Denmark	Aalborg	2.69	4.80	9.17
	Aarhus	2.78	3.57	9.85
	Copenhagen	3.61	4.40	9.21
	Esbjerg	2.95	5.06	9.58
Faroe Islands	Tórshavn	1.94	7.23	7.33
Greenland	Nuuk	2.34	5.00	−0.84
Iceland	Reykjavík	2.12	4.00	5.00
Norway	Bergen	2.24	3.29	8.36
	Oslo	2.67	2.66	6.95
	Stavanger	2.68	4.84	8.56
	Trondheim	2.31	2.32	5.33
Sweden	Gothenburg	2.76	4.23	9.47
	Luleå	2.56	3.21	2.73
	Stockholm	2.85	3.11	7.34
	Umeå	2.68	2.87	3.78

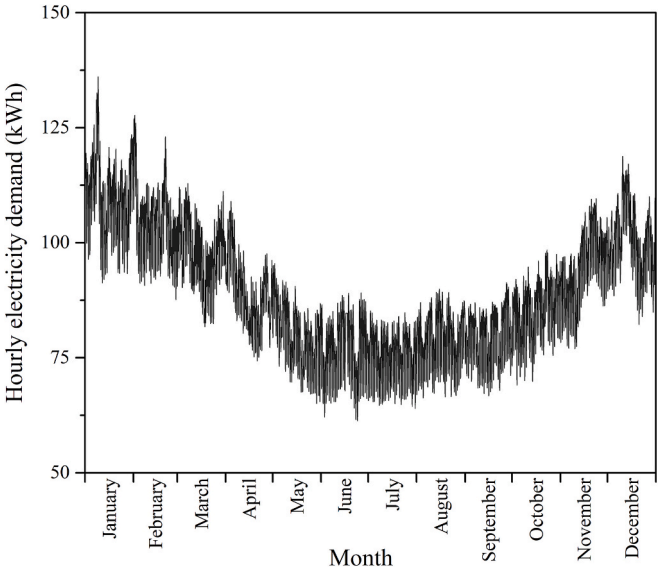

Fig. 2. The hourly electricity demand for 100 persons in Finland.

commissioning, tax, engineering, etc. The inflation (3 %) and nominal discount (4 %) with a project lifetime of 15 years are used to compute the annualised system cost and consequent LCOE. The annualised cost is obtained based on the net present cost and capital recovery factor [63,64]. It should be noted that the initial investment or CAPEX, as well as the operation and maintenance costs or OPEX, are calculated for all the components multiplied by the number of each (N).

$$CAPEX = CAPEX_{WT}N_{WT} + CAPEX_{PV}N_{PV} + CAPEX_{BAT}N_{BAT} + CAPEX_{Inv.}N_{Inv.} \quad (25)$$

$$OPEX = OPEX_{WT}N_{WT} + OPEX_{PV}N_{PV} + OPEX_{BAT}N_{BAT} + OPEX_{Inv.}N_{Inv.} \quad (26)$$

$$NPC = \sum_{i=1}^{n} r(CAPEX + OPEX + REPLACEMENT - SALVAGE) \quad (27)$$

$$C_{annualised} = \frac{r(1+r)^n}{(1+r)^n - 1} NPC \quad (28)$$

Here, $n(year)$ is the lifetime of a project, and $r(\%)$ is the real discount rate. The annual served energy of $E_{served}(kWh/year)$ is only the AC primary load which is supplied by HRES. Therefore, the LCOE ($/kWh) is calculated as follows [65].

$$LCOE = \frac{C_{annualised}}{E_{served}} \quad (29)$$

As can be noticed here, the costs of various components are considered to compute LCOE despite the fact that a huge share of the energy price can be allocated to extra and soft costs in addition to hardware or component costs. These include engineering, permitting, infrastructure, regulatory, administrative, construction, services, losses, and installing or commissioning activities. This value varies for different sizes of microgrid, technology, and location [66]. Here, the share of soft costs is assumed to be 35 % of LCOE on average, which is considered in the energy price calculation [67–69].

Nordic countries are part of Nord Pool, where the electricity price is determined hourly in the day-ahead market. The electricity price is the same for the whole of Finland (FI), while it is divided into four price areas in Sweden (SE1: Luleå in the north, SE2: Sundsvall, SE3: Stockholm, and SE4: Malmö in the south), two in Denmark (DK1: Western Denmark and DK2: Eastern Denmark), and five bidding zones in Norway (NO1: Eastern Norway, NO2: Southern Norway, NO3: Central Norway, NO4: Northern Norway, and NO5: Western Norway). Considering all

these countries and bidding zones, the average electricity market price over the last four years, from January 2021 to June 2025, is 0.08 $/kWh, which is later considered for selling back the surplus electricity in the HRES. However, the electricity price experienced significant variation during this period, reaching as high as three times the current average in 2022 [70].

Although grid connection affects the size of HRES and energy price, two criteria are of great importance, which should be considered, namely the renewable energy tariff and generation at each time step in the studied city [71]. In addition to the spot price and value-added tax, transmission system operators charge consumers for transmitting electricity through the grid, services, infrastructure, etc., which can be diminished in a stand-alone microgrid. The annual average of electricity price in various Nordic bidding zones is summarised in Fig. 3. Only the first half of the year is considered for the average electricity value in 2025. The Unit Transmission Tariff in Europe, which includes TSO expenditure, was about 0.02 $/kWh in 2023 [72].

At the end, uncertainty analysis was done by carrying out a Monte Carlo simulation, which has been used in recent studies in energy systems and uncertainty modelling [73]. Error margins for the LCOE values were estimated, for each case, based on 100,000 Monte Carlo simulations, varying the total optimised capacity for each case by ± 10 %, and by varying the prices of the solar panels, wind energy and batteries, assuming standard deviations of 15 %, 15 % and 25 % respectively. In the Monte Carlo simulations, normal distributions were assumed for each variable.

Results and discussion

PV-WT-DG configuration

In the first exploration, the complete HRES system contains solar (PV) and wind energy (WT), chemical battery storage (BT), a 150-kW biodiesel generator (DG), which covers 10 % more than the peak demand, and a converter to make a connection between AC and DC electrical hubs. The LCOE is demonstrated against wind speed in Fig. 4 for 20 Nordic cities. Tórshavn in the Faroe Islands enjoys the minimum electricity price, storage units, and a converter with an LCOE of 0.16 $/*kWh*, a cumulative battery capacity of 1.38 *MWh*, a converter of 133 kW, and a total wind turbine capacity of 210 kW, together with 313 kW of solar panels in the optimal system. These results indicate that wind energy plays a pivotal role in Nordic regions and could reduce energy

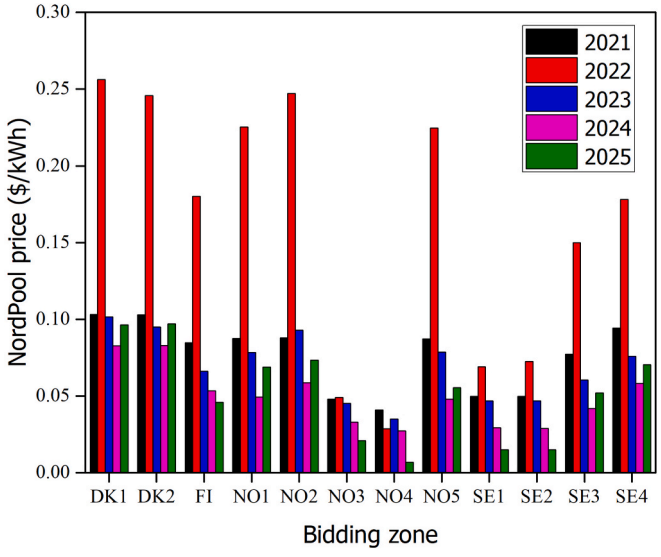

Fig. 3. The average annual Nord Pool electricity price in various Nordic bidding zones [70].

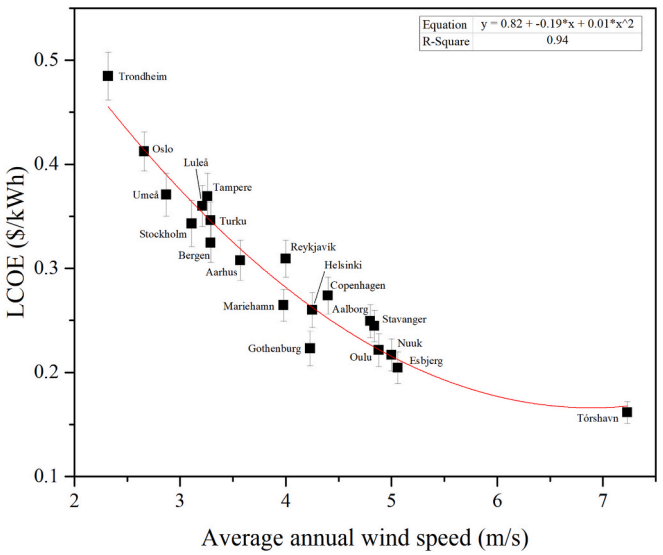

Fig. 4. Levelized component cost of energy ($/kWh) as a function of wind speed (m/s) in medium-sized energy systems consisting of WT/PV/DG/BT/Converter.

prices significantly, and also strongly influence the need for energy storage.

Furthermore, results show that LCOE is at its highest in Trondheim among the investigated cities, with a LCOE, battery, PV, and wind turbine capacity of 0.48 $/*kWh*, 2.81 *MWh*, 1031 *kW*, and 320 *kW* respectively. Generally, the energy price and battery capacity decline with the increase in wind speed, which could cut the LCOE down by 67 % from the highest in Trondheim to the lowest values in Tórshavn among the considered cities. The error margin based on the 100,000 Monte Carlo simulation is demonstrated on the Fig. 4. Cities with higher amounts of wind speed show smaller variability due to the requirement for lower capacity of PV and wind turbines.

To compare results, in a study by Altin [47], HRES, comprising WT/PV/BT, has been investigated, leading to the energy price of 0.16 $/*kWh*, emphasising the significance of correct calculation and usage of wind distribution to achieve realistic wind turbine energy output. Otherwise, the energy price could increase or decrease to 0.23 and 0.14 $/*kWh* in the worst and best scenarios, respectively. Taking 10-kW wind turbines, PV, and battery energy storage into account in Busan, South Korea, the HRES delivered energy at the cost of 0.34 $/*kWh* [74]. This system costs 0.17 $/*kWh* based on wind energy and energy storage, while the cost increased to 0.3 $/*kWh* with WT/DG, excluding the battery units in Gökceada, Turkey [75]. The LCOE of 0.09 $/*kWh* was obtainable in sub-Saharan Africa when PV/DG/BT and a 10-kW wind turbine are integrated into the HRES [76].

As mentioned earlier, 35 % of the final energy price is considered as the soft costs, although it should be noted that taxes, commissioning, engineering, transmission, and regulations vary among those countries, which can significantly affect the final electricity price. Also, if this system were connected to the grid, there would be other installation and grid extension costs, but also other potential revenues, such as selling back the surplus electricity. The surplus electricity could be stored as thermal energy to enhance the system's flexibility and provide heating or cooling capabilities [77].

Generally, less than 1 MW of solar energy capacity is required in the optimum systems with wind energy. With the reduced price of solar panels (and installation costs), the results may differ. The component details of the optimum energy system for each city can be seen in Table 8. Twelve cities encompass only less than 500 kW of PV, and one city necessitates just more than 1 MW of solar panels. Trondheim has the lowest wind speed, leading to the highest energy price. Tampere

Table 8
The details of optimal medium-sized energy systems for 20 cities.

Cities	PV kW	WT kW	DG kW	BT MWh	Converter kW	Dispatch LF/CC	Renewable fraction %
Turku	498	350	150	2.42	153	LF	88.1
Helsinki	322	270	150	2.75	154	LF	93.1
Oulu	242	320	150	2.37	139	LF	95.7
Tampere	508	400	150	3.36	201	LF	89.5
Mariehamn	450	240	150	2.31	140	LF	92.3
Aalborg	513	220	150	2.42	157	LF	94.1
Aarhus	764	230	150	2.75	161	LF	92.5
Copenhagen	715	210	150	2.59	141	LF	94.0
Esbjerg	328	200	150	2.64	139	LF	96.0
Tórshavn	313	210	150	1.38	133	LF	97.2
Nuuk	423	200	150	2.53	138	LF	95.7
Reykjavík	408	270	150	2.86	187	LF	90.5
Bergen	648	260	150	2.81	197	LF	90.7
Oslo	726	310	150	2.42	226	LF	84.1
Stavanger	424	200	150	2.48	140	LF	93.3
Trondheim	1031	320	150	2.81	209	LF	81.9
Gothenburg	313	270	150	2.75	197	LF	96.1
Luleå	473	330	150	3.08	162	LF	88.0
Stockholm	421	480	150	3.03	241	LF	92.0
Umeå	614	360	150	2.97	276	LF	89.0

necessitates the highest amount of energy storage of 3.36 MWH while Stockholm encompasses the highest wind turbine capacity of 480 kW. Although biodiesel generators are an integrated part of the optimal systems in all cities, the renewable fraction is above 81 %. Interestingly, it could be seen that Tórshavn enjoys the lowest amount of LCOE, battery capacity, and biodiesel consumption, which are located in the Faroe Islands, thanks to the high annual wind speed of 7.23 m/s, although it has the lowest solar radiation of 1.94 kW/m^2/day among the investigated cities. This also accentuates again the position of wind energy and this country in wind energy and good capabilities of expanding on– and off-shore wind turbines.

PV-DG configuration, without wind energy

As it is often unfeasible to install wind turbines in small off-grid systems or residential areas, wind turbines are excluded in the second step of the analysis to appraise the HRES consisting of solar energy and a biodiesel generator, together with a storage unit and converter. The optimal LCOE for the investigated cities is illustrated in Fig. 5. Naturally,

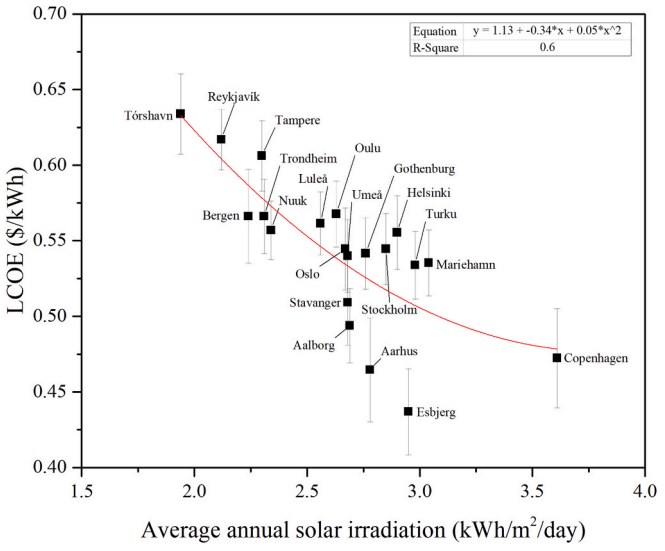

Fig. 5. Levelized component cost of energy ($/kWh) as a function of average annual solar irradiation in medium-sized energy systems consisting of PV/DG/BT/Converter.

the price increases in the absence of wind energy, ranging from 0.44 $/kWh in Esbjerg to 0.63 $/kWh in Tórshavn, while it varies between 0.16 $/kWh in Tórshavn and 0.48 $/kWh in Trondheim in the optimal HRES consisting of wind energy. Furthermore, the energy systems here necessitate a higher amount of storage capacity due to the lack of solar energy during the night and cloudy days. However, the LCOE reduces as the solar irradiation intensity increases, which normally occurs at lower latitudes like in Denmark among the Nordic countries. The variation in solar irradiation leads to 31 % reduction in LCOE among the investigated cities when wind energy is excluded.

However, these calculations demonstrate that there is a potential for HRES in Nordic countries, even without wind energy. To our knowledge, these kinds of results have not been demonstrated earlier for such challenging weather conditions. These systems would not function without biodiesel, but only for a short period of the year. It should be noted that instead of fossil diesel, biodiesel is also currently available in Nordic countries.

The lifetime costs of the different components, including the CAPEX and OPEX of the optimal system, are illustrated in Fig. 6 for Esbjerg (0.44 $/*kWh*) and Tórshavn (0.63 $/*kWh*) with the lowest and highest LCOE, respectively. The high price of energy in Tórshavn is due to its lowest annual solar radiation among 20 cities which is 1.94 kW/m^2/day. Biodiesel generators play a major role in the energy price in Tórshavn due to the more than two times higher amount of fuel consumption than that of Esbjerg. The energy storage is the main contributor to the LCOE in Bergen, with the highest storage capacity of 4.13 MWh. The lowest renewable fraction here is 57 % in Reykjavík, with the highest amount of biodiesel consumption among the studied cases. Further hybridisation and taking advantage of alternative renewable resources, such as hydrogen and electrolysers, is clearly motivated in Tórshavn, Reykjavík, and other cities with a high share of biodiesel to achieve higher energy security, sustainability, and reliability.

In these systems, Fig. 7 and Fig. A. 1 represent the average monthly electricity generation by the biodiesel generator in red and solar panels in green, together with the amount of battery and PV capacity. The energy demand is demonstrated in the dotted line to distinguish between the load and surplus energy, which is underneath and above the dotted line, respectively. As a typical phenomenon in renewable energy systems, all cases produce significant surplus electricity during long days of sunshine almost from March to October, which could be harnessed to improve the system efficiency and reduce emissions and energy costs by utilizing in other applications such as generating hydrogen as a promising way of storing energy, heating and cooling system, selling to the

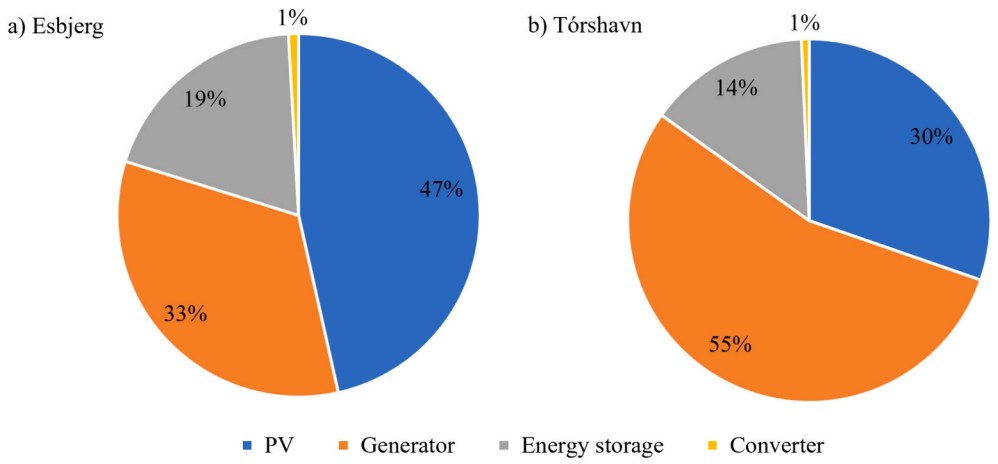

Fig. 6. The total cost comparison of various components (CAPEX and OPEX) of the optimal system in a) Esbjerg with the lowest LCOE and b) Tórshavn with the highest LCOE in the HRES without wind energy.

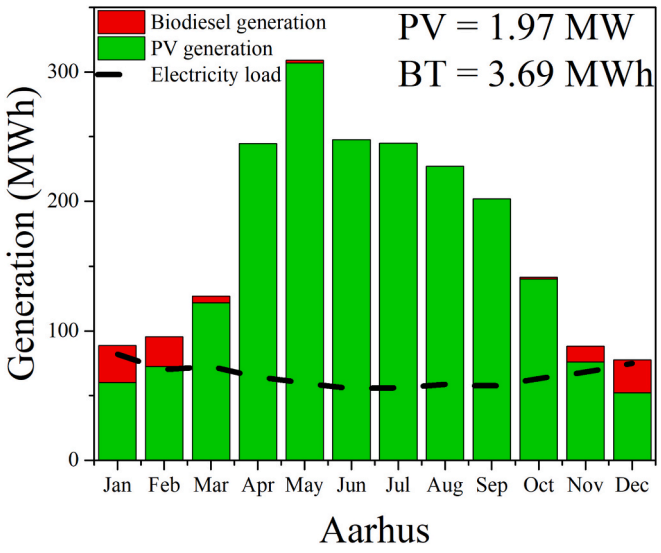

Fig. 7. The electricity generation by various components in optimum HRES in Aarhus, including PV/BT/DG/Converter. The dotted line displays the average monthly electricity load.

electricity grid, to name but a few. The average Nord Pool electricity price in various zones based on the Fig. 3 could be used to estimate the revenue from the surplus electricity if grid connection and feed-in tariff is possible.

The results show that the maximum amount of energy, which is 2095 *MWh*, is generated annually in Aarhus (Fig. 7) and peaks at 307 *MWh* by solar panels in May, while the electricity demand is 60 *MWh* in the same month. This outcome affirms the crucial role of solar energy, especially during the summertime, in Nordic countries despite having dark, cloudy, freezing climatic conditions during long-lasting winters. The PV generation can become as low as 0.4 *MWh* in December, from its highest value of 124.5 *MWh* in May in Reykjavík. More surprisingly, solar energy alone is enough to meet the electricity demand between May and August in 9 cities and with the trivial help of a biodiesel generator in the rest of the cities. In a study by Lau et al. in Malaysia [78], PV/DG/BT-based HRES achieved the lowest energy price of 0.57 $, /*kWh* considering the annual real interest rate of 6 %. In Gökceada, Turkey [75], PV/DG/BT and PV/DG HRESs delivered energy at 0.63 and 0.75 $/*kWh*, respectively. The energy rate for this combination of PV/DG/BT was shown to be around 0.35 $/*kWh* while changing a little with interest rates [79]. The PV/DG/BT, excluding WT, demonstrates its superiority in energy prices for areas that enjoy an acceptable amount of solar radiation in Mukalla, Yemen, but less wind energy compared to the Nordics, with the LCOE of 0.13 $/*kWh* [80].

PV configuration, without biodiesel and wind energy

In the last step, a diesel generator is also eliminated from the studied HRES to highlight the role of solar energy as one of the accessible and socially accepted renewable sources of energy, which could be easily installed on the rooftop. In this case, cities located in Denmark enjoy the lowest amount of storage capacity and LCOE, even without wind and biodiesel energy. This is because Denmark is located at a lower latitude and generally receives a higher amount of solar irradiation than other explored cities. This will highlight Denmark's position not only in wind energy in the world but also in solar energy among Nordic countries.

Although the electricity demand could be met by only solar energy, it should be noted that the optimum system includes a significantly huge amount of PV and battery energy storage, which pushes the LCOE, PV size, and battery capacity to be as high as 3.35 $/*kWh* in Nuuk, 14.82 *MW* in Umeå, and 109.23 *MWh* in Reykjavík respectively. The LCOE can reduce 76.1 % from its highest value of 3.35 $/kWh in Nuuk to its lowest value of 0.80 $/kWh in Aarhus. This is while the maximum required solar panel capacity was 1.98 *MW* in Copenhagen in PV/DG/BT and 1.03 *MW* in Trondheim in the optimum WT/PV/DG/BT HRES. The price of PV-based systems generally reduces in countries with stronger solar irradiation and lower latitudes, such as 0.11 $/*kWh* in Palestine [81].

The variation of LCOE against the average annual solar irradiation and battery capacity is illustrated in Fig. 8 and Fig. 9, respectively. As can be seen, the LCOE increases for the systems requiring a higher amount of storage capacity, leading also to the higher variation in error margins based on the Monte Carlo calculation. These cities typically are located at higher latitudes with a lower amount of solar irradiation compared to cities located in Denmark at lower latitudes with a higher amount of sunshine, when wind energy is excluded. Typically, LCOE decreases as the solar intensity surges while demanding less storage capacity. Although the adoption of a fully PV/BBT-based system is possible, the optimal energy cost is achieved not only by the appropriate level of PV capacity but also by the trade-off between solar energy and energy storage capacity [82]. Studying PV-based energy systems in Turkey [75], the energy cost was 1.2 $/*kWh*. This price was even higher for the PV/BT energy system in the north of Algeria, with the energy cost of 6.9 $/*kWh* [83].

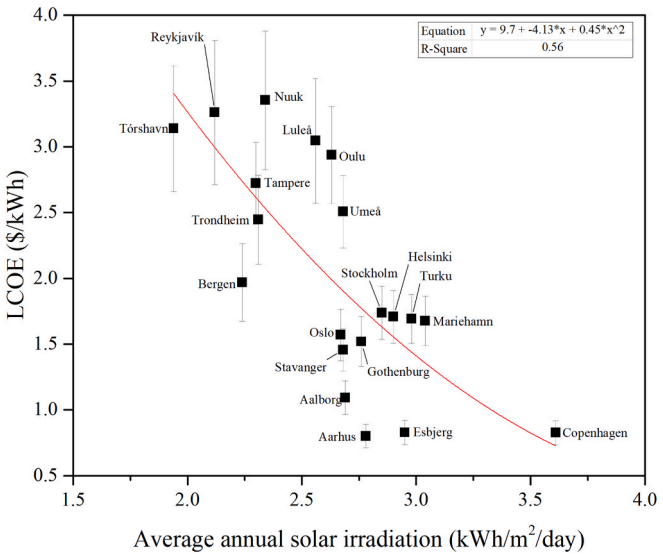

Fig. 8. Levelized component cost of energy ($/kWh) as a function of average annual solar irradiation in medium-sized energy systems consisting of PV/BT/Converter.

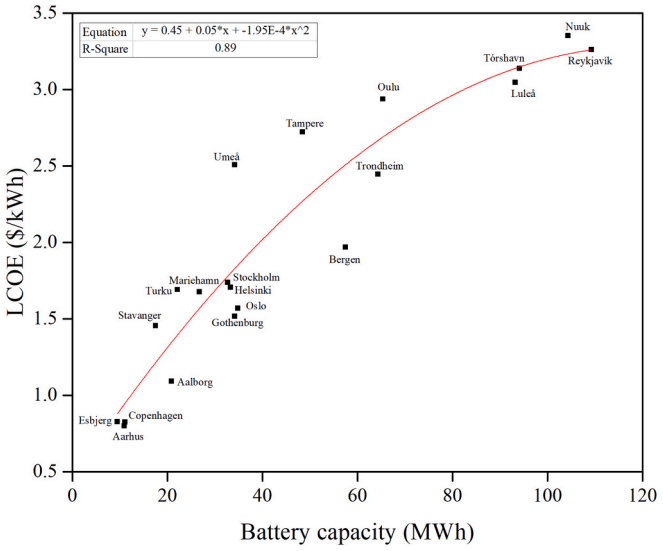

Fig. 9. Levelized component cost of energy ($/kWh) as a function of battery capacity in medium-sized energy systems consisting of PV/BT/Converter.

Battery degradation

The battery capacity, power, and voltage deteriorate over the lifetime of the project. The storage capacity degrades over time due to the cycle and calendar ageing, which are assumed to be the main elements of the Li-ion battery degradation mechanism [84]. The battery decay process exacerbates not only at high working temperatures but also at low and high states of the charge [85]. Here, HRESs with the largest storage capacity are considered to examine the effect of battery degradation on the energy price. Two degradation rates of 1 % and 2 % are considered, which lead to the overall capacity reduction of 16 % and 35 % over the project lifetime of 15 years. To simplify the calculation, the energy system is modelled with the higher capacity of storage units equal to the capacity decrease over 15 years, while other parameters remain constant. According to the results in Table 9, HRESs with and without wind energy deliver electricity at around 5 % higher electricity price in the worst case, with the highest storage capacity and degradation of 2 %. This is while 13.7 % and 30.2 % higher LCOE is observable in PV-based systems with 1 % and 2 % battery degradation, respectively. These differences in Reykjavík are due to the high amount of battery storage, which is 147.89 MWh. Therefore, battery degradation plays a significant role in HRES, and more specifically in systems with a high capacity for energy storage.

Sensitivity analysis

The technology is regularly and rapidly improving, which significantly affects component prices and efficiency. Here, the effect of the price decline in batteries, wind turbines, and photovoltaics sheds light on the possible variation in the LCOE in the foreseeable future. To perform this sensitivity analysis, the systems with the highest energy price are considered to investigate the effect of component costs on LCOE. The sensitivity analysis is done for Trondheim, with the LCOE of 0.48 $/kWh, Tórshavn with LCOE of 0.63 $/kWh, and Nuuk with LCOE of 3.35 $/kWh in an optimal energy system of WT/DG/PV/BT, DG/PV/BT, and PV/BT, respectively. In this analysis, all prices are kept constant except the targeted parameter in each case, namely, wind turbine, solar panel, and battery capital and replacement costs. The WT, PV, and BT prices are assumed to be reduced by 25 %, 50 %, 75 %, and 90 % corresponding to the price multiplier of 0.75, 0.50, 0.25, and 0.90.

The LCOE alternation with the costs of battery and PV is illustrated in Fig. 10 for Trondheim and Tórshavn, and in Fig. 11 for Nuuk. The energy price in Trondheim and Tórshavn is more dependent on PV prices than battery prices, while the opposite is true in Nuuk. In Trondheim with wind energy, the results show a higher dependency of LCOE on wind turbine price than that of battery. The LCOE reduction is generally the same in regards to PV price decline in these three cities, where the differences are marginal. Almost a 10 % decrease in LCOE is possible with a 50 % decrease in PV price in three cases. However, the largest effect of PV price occurs in Tórshavn in a PV/DG/BT configuration. The highest impact is seen in battery price variation in Nuuk with PV-based HRES, where the optimal systems require a significant amount of energy storage units. Energy price falls about 5 % in Trondheim and Tórshavn if the battery price declines by 50 %. This is while 31 % less LCOE is possible by a 50 % battery price reduction. More than 7 % energy price variation could be expected by a 50 % change in the cost of the wind turbine in Trondheim. The more comprehensive results of the sensitivity analysis are observable in Table A. 1.

As was mentioned earlier, the LCOE of Nuuk has a higher correlation with battery price (Fig. 11) than that of PV, as LCOE reduces by 56 % and 16 % when the battery costs 90 % and 25 % less than the current one. This is since there is a higher amount of storage units in the optimum

Table 9
The battery degradation results for cities with the highest amount of battery capacity in each HRES configuration.

Tampere (with wind energy)	0 % degradation		1 % degradation		2 % degradation	
	Base battery capacity (MWh)	LCOE ($/kWh)	16 % higher storage (MWh)	LCOE ($/kWh)	35 % higher storage (MWh)	LCOE ($/kWh)
Tampere (with wind energy)	3.36	0.37	3.9	0.37	4.54	0.38
Bergen (without wind energy)	4.13	0.57	4.80	0.58	5.59	0.6
Reykjavík (only PV)	109.23	3.26	127	3.71	147.89	4.25

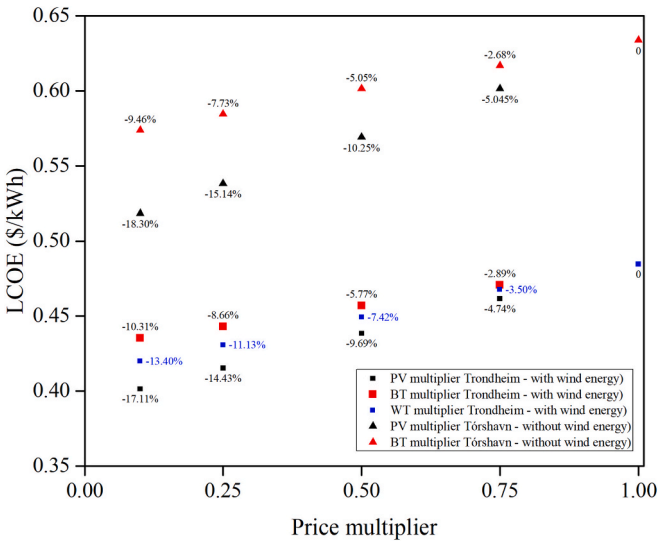

Fig. 10. The effect of PV price multiplier in black, battery price multiplier in red, and WT price multiplier in blue on LCOE in Reykjavík without WT and Oslo with WT. (For interpretation of the references to colour in this figure legend, the reader is referred to the web version of this article.)

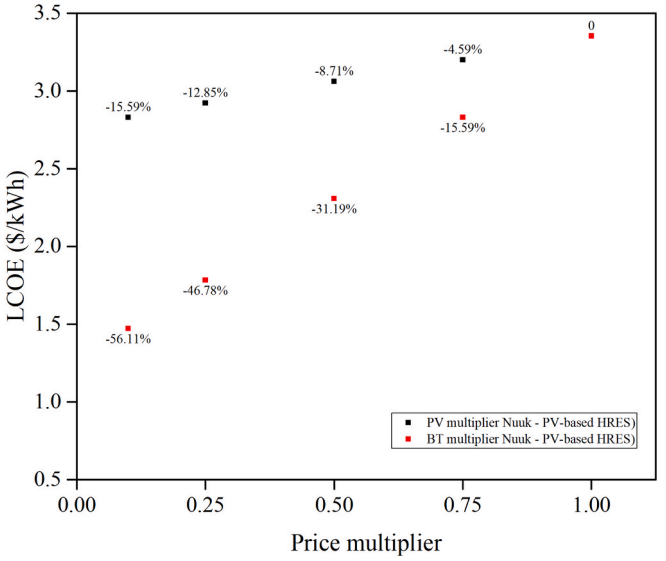

Fig. 11. The effect of PV price multiplier in black and battery price multiplier in red on LCOE in Nuuk (PV-based HRES). (For interpretation of the references to colour in this figure legend, the reader is referred to the web version of this article.)

PV/BT energy system than in other cases, with 104.34 *MWh* energy storage capacity in Nuuk compared to 3.36 *MWh* in Tórshavn or 2.81 *MWh* in Trondheim.

Limitations and constraints

Although hourly climatic data is used, the weather conditions are generally different in various not only times but also locations or the location of meteorological institutes. Therefore, it is of great importance to measure the specific location data at a reliable time to reduce uncertainties. It is of pivotal significance to employ the reliable and appropriate models to complete the data when data is missing or incomplete. It could be useful to average data from different measurement spots to have more reliable figures.

Due to technological development and advancement, the price of components varies rapidly over the years, which affects the energy price. These price variations also occur as a result of natural disasters, strikes, war, conflict between countries, etc. Moreover, the fixed amount of discount rate, bio-fuels, and inflation are examined, which is not the case in real life. Therefore, it is necessary to update such studies over time to achieve more realistic results, especially for investment and policymaking purposes. The average soft and extra costs are considered here based on the reports and literature, which vary significantly for different kinds of projects, depending on the location, size of the project, and technologies. Therefore, it is of pivotal importance to take project-specific data into account to achieve a precise price.

It should be noted that some assumptions and simplifications have been used for calculation and optimisation, which may not fully model the real situation, and further study should be performed to validate the results or correctly adjust the model parameters. National or regional regulations, environmental issues, social impacts and acceptance, political situation, permitting, land use, incentives, and so on should be considered for better evaluation of the project as well.

The reliable result of an optimisation in a real project is essential for further study and power system integration (grid-connected HRES), as energy losses, voltage deterioration, and power fluctuation in the grid impose serious damage to the power network and the quality of the energy. Therefore, the optimisation algorithm and reliable data play a significant role when it comes to voltage stability and an on-grid microgrid requiring continuous improvement in optimisation and integration models [86]. This is even more important in distributed energy systems coupled with renewable energy sources due to the inherent intermittency of renewables.

Conclusion

The present study investigated the role of wind and solar irradiation on the cost of medium-sized energy systems (for 100 persons) in 20 cities in Nordic countries. In these cities, the average (throughout the year) wind speed varies between 2.32 and 7.23 m/s, and the solar irradiation varies from 1.94 to 3.61 kWh/m^2/day. The optimised systems consist of small-scale wind energy, solar energy, batteries, and biodiesel generators (as backup energy). More than 500,000 data points were used in the optimisation.

The results show that the costs of the optimised systems decrease as functions of increased average wind speed and increased solar irradiation. For the optimised systems with wind energy, the results show that the levelized costs (for a 15-year period) range between 0.16 and 0.48 $/kWh. The results exhibit a high correlation with wind speed under the investigated conditions, with the lowest energy prices occurring at the highest wind speed. For the optimised systems without wind energy, the cost ranges from 0.44 to 0.63 $/kWh. Relying solely on solar energy and energy storage leads to an energy price of between 0.80 and 3.35 $/kWh.

These results clarified how wind energy and solar irradiation influence the configuration and cost of medium-sized energy systems under challenging weather conditions. Further, the study indicates that medium-sized off-grid hybrid energy systems (HRES) have strong potential even in countries with long winters but satisfactory daylight during summer times.

CRediT authorship contribution statement

MohammadReza Akhtari: Writing – original draft, Visualization, Validation, Software, Methodology, Investigation, Funding acquisition, Formal analysis, Data curation, Conceptualization. **Oskar Karlström:** Writing – review & editing, Supervision, Project administration, Methodology, Funding acquisition, Conceptualization.

Declaration of competing interest

The authors declare that they have no known competing financial interests or personal relationships that could have appeared to influence the work reported in this paper.

Acknowledgement

We want to acknowledge the University of Turku Graduate School (UTUGS) for financial support, and we also want to acknowledge the Business Finland co-innovation project Data-Driven Sustainability Management.

Appendix A

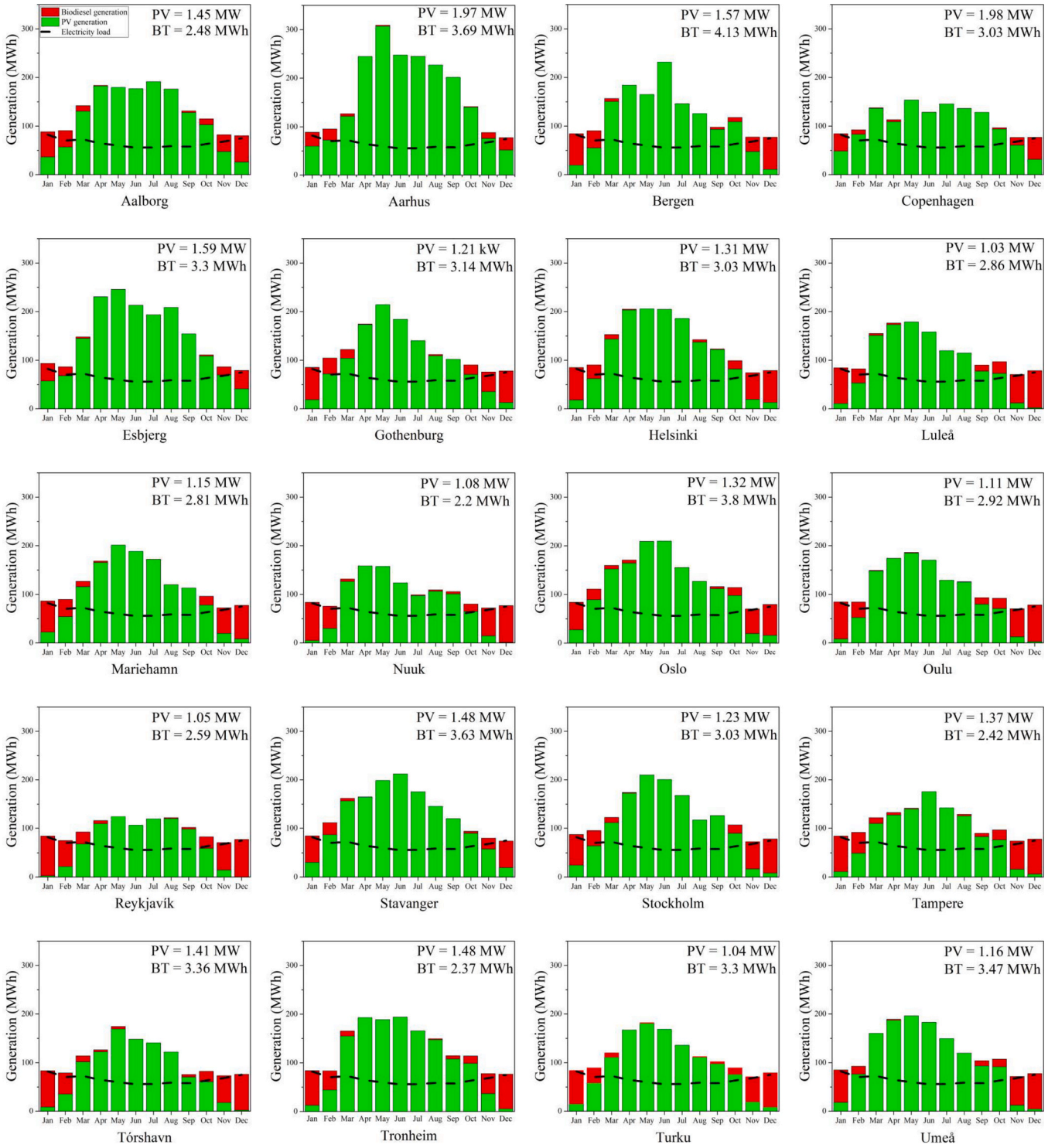

Fig. A1. The average monthly electricity generation by PV and DG in optimum HRES, including PV/BT/DG/Converter. The dotted line displays the average monthly electricity demand.

Table A1
Sensitivity analysis for Trondheim with wind energy, Tórshavn without wind energy, and Nuuk in a PV-based HRES. The optimum cases with the highest LCOE are selected in each configuration of HRES for sensitivity analysis.

WT		PV		BT		LCOE
Multiplier	$/kW	Multiplier	$/kW	Multiplier	$/kWh	$/kWh
Trondheim	**WT/PV/BT/DG/Converter**					
1	200	1	950	1	180	0.49
0.75	150	1	950	1	180	0.47
0.5	100	1	950	1	180	0.45
0.25	50	1	950	1	180	0.43
0.1	20	1	950	1	180	0.42
1	200	0.75	712.5	1	180	0.46
1	200	0.5	475	1	180	0.44
1	200	0.25	237.5	1	180	0.42
1	200	0.1	95	1	180	0.40
1	200	1	950	0.75	135	0.47
1	200	1	950	0.5	90	0.46
1	200	1	950	0.25	45	0.44
1	200	1	950	0.1	18	0.44
Tórshavn	**PV/BT/DG/Converter**					
		1	950	1	180	0.63
		0.75	712.5	1	180	0.60
		0.5	475	1	180	0.57
		0.25	237.5	1	180	0.54
		0.1	95	1	180	0.52
		1	950	0.75	135	0.62
		1	950	0.5	90	0.60
		1	950	0.25	45	0.59
		1	950	0.1	18	0.57
Nuuk	**PV/BT/Converter**					
		1	950	1	180	3.35
		0.75	712.5	1	180	3.20
		0.5	475	1	180	3.06
		0.25	237.5	1	180	2.92
		0.1	95	1	180	2.83
		1	950	0.75	135	2.83
		1	950	0.5	90	2.31
		1	950	0.25	45	1.79
		1	950	0.1	18	1.47

Data availability

Data will be made available on request.

References

[1] IRENA (2025). Renewable capacity statistics 2025, International Renewable Energy Agency, Abu Dhabi. n.d. https://www.irena.org/Publications/2025/Mar/Renewable-capacity-statistics-2025.
[2] IEA (2023). World Energy Outlook 2023, IEA, Paris https://www.iea.org/reports/world-energy-outlook-2023, Licence: CC BY 4.0 (report); CC BY NC SA 4.0 (Annex A). n.d.
[3] Barney A, Petersen UR, Polatidis H. Energy scenarios for the Faroe Islands: a MCDA methodology including local social perspectives. Sustain Futures 2022;4:100092. https://doi.org/10.1016/j.sftr.2022.100092.
[4] IEA, Energy mix, Electricity generation 2022. https://www.iea.org/countries.
[5] Quirk DG, Mendonça F, Henriques F, Jørgensen T, Lahtimo M, Figueira A, et al. Energy transition league: a comparison of islands' paths to net zero emissions n.d.
[6] Lindberg MB. The power of power markets: zonal market designs in advancing energy transitions. Environ Innov Soc Transit 2022;45:132–53. https://doi.org/10.1016/j.eist.2022.08.004.
[7] Analysing DNN. Interpretability and Accuracy in Electricity Price Forecasting n.d.
[8] Hirvonen J, Sirén K. A novel fully electrified solar heating system with a high renewable fraction – optimal designs for a high latitude community. Renew Energy 2018;127:298–309. https://doi.org/10.1016/j.renene.2018.04.028.
[9] Hirvonen J, ur Rehman H, Sirén K. Techno-economic optimization and analysis of a high latitude solar district heating system with seasonal storage, considering different community sizes. Sol Energy 2018;162:472–88. https://doi.org/10.1016/j.solener.2018.01.052.
[10] Lundheim SH, Vesely S, Nayum A, Klöckner CA. From vague interest to strong intentions to install solar panels on private homes in the North – an analysis of psychological drivers. Renew Energy 2021;165:455–63. https://doi.org/10.1016/j.renene.2020.11.034.
[11] WindEurope. Wind energy in Europe: 2024 Statistics and the outlook for 2025-2030 n.d. https://windeurope.org/intelligence-platform/product/wind-energy-in-europe-2024-statistics-and-the-outlook-for-2025-2030/ (accessed May 20, 2025).
[12] European Commission. European Climate Law n.d. https://climate.ec.europa.eu/eu-action/european-climate-law_en (accessed July 1, 2025).
[13] Nordic Council of Ministers. Policy Brief: Nordic Stocktake and Visions – Pathways to Climate Neutrality n.d. https://pub.norden.org/nord2023-037/climate-neutrality-targets-in-the-nordic-region.html?utm_source=chatgpt.com (accessed July 1, 2025).
[14] Satymov R, Bogdanov D, Galimova T, Breyer C. Energy and industry transition to carbon-neutrality in Nordic conditions via local renewable sources, electrification, sector coupling, and power-to-X. Energy 2025;319:134888. https://doi.org/10.1016/j.energy.2025.134888.
[15] Nordic Council of Ministers. Activities – Nordic Energy Research n.d. https://www.nordicenergy.org/projects/ (accessed July 1, 2025).
[16] Ćosić B, Duić N. Impact of the EU carbon border adjustment mechanism and variable renewable energy integration on fossil-based energy systems. Energy Convers Manage: X 2025;26:101008. https://doi.org/10.1016/j.ecmx.2025.101008.
[17] Hyvönen J, Koivunen T, Syri S. Review of climate strategies in Northern Europe: exposure to potential risks and limitations. Energies (Basel) 2024;17:1538.
[18] European Commission. Strategy and policy n.d. https://commission.europa.eu/strategy-and-policy_en (accessed July 1, 2025).
[19] Rinne S, Syri S. The possibilities of combined heat and power production balancing large amounts of wind power in Finland. Energy 2015;82:1034–46. https://doi.org/10.1016/j.energy.2015.02.002.

[20] Hedegaard K, Meibom P. Wind power impacts and electricity storage – a time scale perspective. Renew Energy 2012;37:318–24. https://doi.org/10.1016/j.renene.2011.06.034.
[21] Meriläinen A, Montonen J-H, Hopsu J, Kosonen A, Lindh T, Ahola J. Power balance control and dimensioning of a hybrid off-grid energy system for a Nordic climate townhouse. Renew Energy 2023;209:310–24. https://doi.org/10.1016/j.renene.2023.03.104.
[22] WindEurope Intelligence Platform | WindEurope 2024. https://windeurope.org/intelligence-platform.
[23] Jurasz J, Bochenek B, Wieczorek J, Jaczewski A, Kies A, Figurski M. Energy potential and economic viability of small-scale wind turbines. Energy 2025;322:135608. https://doi.org/10.1016/j.energy.2025.135608.
[24] McKenna R, Lilliestam J, Heinrichs HU, Weinand J, Schmidt J, Staffell I, et al. System impacts of wind energy developments: Key research challenges and opportunities. Joule 2025;9. https://doi.org/10.1016/j.joule.2024.11.016.
[25] Dimd BD, Völler S, Cali U, Midtgård O-M. A review of machine learning-based photovoltaic output power forecasting: Nordic context. IEEE Access 2022;10:26404–25. https://doi.org/10.1109/ACCESS.2022.3156942.
[26] Rehman H, ur Hasan A, Reda F. Challenges in reaching positive energy building level in apartment buildings in the Nordic climate: a techno-economic analysis. Energ Buildings 2022;262:111991. https://doi.org/10.1016/j.enbuild.2022.111991.
[27] The Energy Transition in 2025: What to Watch For - RMI n.d. https://rmi.org/the-energy-transition-in-2025-what-to-watch-for/ (accessed March 4, 2025).
[28] Global Cost of Renewables to Continue Falling in 2025 as China Extends Manufacturing Lead: BloombergNEF | BloombergNEF n.d. https://about.bnef.com/blog/global-cost-of-renewables-to-continue-falling-in-2025-as-china-extends-manufacturing-lead-bloombergnef/ (accessed March 4, 2025).
[29] Akhtari MR, Shayegh I, Karimi N. Techno-economic assessment and optimization of a hybrid renewable earth – air heat exchanger coupled with electric boiler, hydrogen, wind and PV configurations. Renew Energy 2020;148:839–51. https://doi.org/10.1016/j.renene.2019.10.169.
[30] Akhtari M, Karlström O. Techno-economic assessment of hybrid renewable energy system: case studies in Nordic countries. In: 2024 9th International Youth Conference on Energy (IYCE). IEEE; 2024. p. 1–6. https://doi.org/10.1109/IYCE60333.2024.10634937.
[31] Thirunavukkarasu M, Sawle Y, Lala H. A comprehensive review on optimization of hybrid renewable energy systems using various optimization techniques. Renew Sustain Energy Rev 2023;176:113192. https://doi.org/10.1016/J.RSER.2023.113192.
[32] Maleki Tehrani M, Akhtari M, Kasaeian A, Vaziri Rad MA, Toopshekan A, Sadeghi MM. Techno-economic investigation of a hybrid biomass renewable energy system to achieve the goals of SDG-17 in deprived areas of Iran. Energy Convers Manag 2023;291:117319. https://doi.org/10.1016/J.ENCONMAN.2023.117319.
[33] Muthusamy Suresh, Meenakumari R. Software tools for analyzing the integration of various renewable energy systems. Int J Ind Eng 2018:135–40.
[34] Agajie TF, Ali A, Fopah-Lele A, Amoussou I, Khan B, Velasco CLR, et al. A comprehensive review on techno-economic analysis and optimal sizing of hybrid renewable energy sources with energy storage systems. Energies 2023;16:642. https://doi.org/10.3390/EN16020642.
[35] Ram K, Swain PK, Vallabhaneni R, Kumar A. Critical assessment on application of software for designing hybrid energy systems. Mater Today Proc 2022;49:425–32. https://doi.org/10.1016/J.MATPR.2021.02.452.
[36] Silinto BF, van der Laag YC, Zuidema C, Faaij APC. Hybrid renewable energy systems for rural electrification in developing countries: a review on energy system models and spatial explicit modelling tools. Renew Sustain Energy Rev 2025;207:114916. https://doi.org/10.1016/j.rser.2024.114916.
[37] Rahimi I, Li M, Choon J, Pamuspusan D, Huang Y, He B, et al. Optimizing renewable energy site selection in rural Australia: clustering algorithms and energy potential analysis. Energy Convers Manage: X 2025;25:100855. https://doi.org/10.1016/j.ecmx.2024.100855.
[38] Ember. Global Electricity Review 2025 n.d. https://ember-energy.org/latest-insights/global-electricity-review-2025/.
[39] Burton T, Jenkins N, Sharpe D, Bossanyi E. Wind energy handbook. John Wiley & Sons; 2011.
[40] Nawaz Khan S, Ali Abbas Kazmi S. Integrative decision-making framework for techno-economic planning and sustainability assessment of renewable dominated standalone hybrid microgrids infrastructure at provincial scale of Pakistan. Energy Convers Manag 2022;270:116168. https://doi.org/10.1016/j.enconman.2022.116168.
[41] Duffie JA, Beckman WA, Blair N. Solar engineering of thermal processes, photovoltaics and wind. John Wiley & Sons; 2020.
[42] Suganthi D, Jamuna K. Optimizing campus microgrid energy systems: Economic, environmental, and sensitivity insights. Energy Convers Manage: X 2025;27:101046. https://doi.org/10.1016/j.ecmx.2025.101046.
[43] Duffie JA, Beckman WA, McGowan J. Solar engineering of thermal processes. Am J Phys 1985;53:382. https://doi.org/10.1119/1.14178.
[44] Baidya H, Rahman Zisan MT, Alif AZ, Ahmed A, Hasan M, Chowdhury N-U-R. Techno-economic comparative analysis of hybrid renewable energy systems optimization considering off-grid remote area electrification in Bangladesh. Energy Convers Manage: X 2025;26:101004. https://doi.org/10.1016/j.ecmx.2025.101004.
[45] Manwell JF, McGowan JG. Lead acid battery storage model for hybrid energy systems. Sol Energy 1993;50:399–405. https://doi.org/10.1016/0038-092X(93)90060-2.
[46] Heidari M, Heidari M, Soleimani A, Mehdizadeh Khorrami B, Pinnarelli A, Vizza P, et al. Techno-economic optimization and Strategic assessment of sustainable energy solutions for Powering remote communities. Results Eng 2024;23:102521. https://doi.org/10.1016/j.rineng.2024.102521.
[47] Altin C. Investigation of the effects of synthetic wind speed parameters and wind speed distribution on system size and cost in hybrid renewable energy system design. Renew Sustain Energy Rev 2024;197:114420. https://doi.org/10.1016/j.rser.2024.114420.
[48] Araoye TO, Ashigwuike EC, Mbunwe MJ, Bakinson OI, Ozue TI. Techno-economic modeling and optimal sizing of autonomous hybrid microgrid renewable energy system for rural electrification sustainability using HOMER and grasshopper optimization algorithm. Renew Energy 2024;229:120712. https://doi.org/10.1016/j.renene.2024.120712.
[49] Solar Electric Supply Inc. Canadian Solar CS6X-325P Solar Panel n.d. https://www.solarelectricsupply.com/canadian-solar-cs6x-325p-solar-panel-325-watt-max-power (accessed May 16, 2025).
[50] Spataru C, Bouffaron P. Chapter 22 – off-grid energy storage. In: Letcher TM, editor. Storing Energy. Oxford: Elsevier; 2016. p. 477–97. https://doi.org/10.1016/B978-0-12-803440-8.00022-1.
[51] Clean Energy Institute (University of Washington). Lithium-Ion Battery n.d. https://www.cei.washington.edu/research/energy-storage/lithium-ion-battery/?utm_source=chatgpt.com (accessed July 9, 2025).
[52] Dhundhara S, Verma YP, Williams A. Techno-economic analysis of the lithium-ion and lead-acid battery in microgrid systems. Energy Convers Manag 2018;177:122–42. https://doi.org/10.1016/j.enconman.2018.09.030.
[53] Killer M, Farrokhseresht M, Paterakis NG. Implementation of large-scale Li-ion battery energy storage systems within the EMEA region. Appl Energy 2020;260:114166. https://doi.org/10.1016/j.apenergy.2019.114166.
[54] The International Energy Agency (IEA). Norway – Countries & Region n.d. https://www.iea.org/countries/norway (accessed May 19, 2025).
[55] Finnish Meteorological Institute (FMI) n.d. https://en.ilmatieteenlaitos.fi/download-observations (accessed July 14, 2025).
[56] Danish Meteorological Institute (DMI) n.d. https://opendatadocs.dmi.govcloud.dk/en/DMIOpenData (accessed July 16, 2025).
[57] Norwegian Centre for Climate Services n.d. https://seklima.met.no/ (accessed July 14, 2025).
[58] Photovoltaic Geographical Information System (PVGIS) n.d. https://re.jrc.ec.europa.eu/pvg_tools/en/#HR (accessed July 15, 2025).
[59] Icelandic Meteorological Office (IMO) n.d. https://en.vedur.is/climatology/data/ (accessed July 16, 2025).
[60] NASA POWER n.d. https://power.larc.nasa.gov/data-access-viewer/ (accessed July 15, 2025).
[61] Fingrid Oyj. Finland's transmission system operator n.d. https://www.fingrid.fi/en/.
[62] Yadav S, Kumar P, Kumar A. Techno-economic assessment of hybrid renewable energy system with multi energy storage system using HOMER. Energy 2024;297:131231. https://doi.org/10.1016/j.energy.2024.131231.
[63] Nassar YF, El-Khozondar HJ, Fakher MA. The role of hybrid renewable energy systems in covering power shortages in public electricity grid: an economic, environmental and technical optimization analysis. J Energy Storage 2025;108:115224. https://doi.org/10.1016/j.est.2024.115224.
[64] Irshad AS, Ahmadullah AB, Kamal K, Haidari N, Qanit A, Osmani JA, et al. Optimization of coal sustainability via hybrid renewable integration: a PVsyst-HOMER synergistic framework for sustainable energy transitions. Energy Convers Manage: X 2025;27:101110. https://doi.org/10.1016/j.ecmx.2025.101110.
[65] Roy D, Wang R, Roy S, Smallbone A, Roskilly AP. Hybrid renewable energy systems for sustainable power supply in remote location: techno-economic and environmental assessment. Energy Convers Manage: X 2024;24:100793. https://doi.org/10.1016/j.ecmx.2024.100793.
[66] IRENA (2024). Renewable power generation costs in 2023, International Renewable Energy Agency, Abu Dhabi 2024. https://www.irena.org/Publications/2024/Sep/Renewable-Power-Generation-Costs-in-2023 (accessed June 26, 2025).
[67] Giraldez Miner JI, Flores-Espino F, MacAlpine S, Asmus P. Phase I microgrid cost study: Data collection and analysis of microgrid costs in the United States. Golden, CO (United States): National Renewable Energy Lab (NREL); 2018.
[68] Sustainability Directory. What Are Microgrid Costs for Diverse Applications? 2025. https://sustainability-directory.com/question/what-are-microgrid-costs-for-diverse-applications/ (accessed June 26, 2025).
[69] Lugo-Laguna D, Arcos-Vargas A, Nuñez-Hernandez F. A European assessment of the solar energy cost: key factors and optimal technology. Sustainability 2021;13. https://doi.org/10.3390/su13063238.
[70] Nord Pool. Day-ahead prices n.d. https://data.nordpoolgroup.com/auction/day-ahead/prices?deliveryDate=latest&currency=EUR&aggregation=YearlyAggregate&deliveryAreas=AT,DK1,DK2,FI,FRE,NO1,NO2,NO3,NO4,NO5,SE,SE1,SE2,SE3,SE4 (accessed June 26, 2025).
[71] Mousavi S, Jahangir MH, Kasaeian A. A decision-making method for optimal sizing of a sustainable residential building via a multi-objective optimization method. Energy Convers Manage: X 2025;26:101002. https://doi.org/10.1016/j.ecmx.2025.101002.
[72] ENTSO-E. Overview of Transmission Tariffs in Europe for 2022 and 2023 n.d. https://www.entsoe.eu/news/2025/06/20/entso-e-publishes-its-annual-overview-of-transmission-tariffs-in-europe-for-2022-and-2023/ (accessed July 3, 2025).
[73] Megantoro P, Al-Humairi SNS, Ma'arif A, Nugraha YU, Prastio RP, Awalin LJ, et al. Modeling the uncertainties and active power generation of wind-solar energy with data acquisition from telemetry weather measurement. Results Eng 2025;25:104392. https://doi.org/10.1016/j.rineng.2025.104392.

[74] Baek S, Park E, Kim M-G, Kwon SJ, Kim KJ, Ohm JY, et al. Optimal renewable power generation systems for Busan metropolitan city in South Korea. Renew Energy 2016;88:517–25. https://doi.org/10.1016/J.RENENE.2015.11.058.
[75] Demiroren A, Yilmaz U. Analysis of change in electric energy cost with using renewable energy sources in Gökceada, Turkey: an island example. Renew Sustain Energy Rev 2010;14:323–33. https://doi.org/10.1016/J.RSER.2009.06.030.
[76] Samatar AM, Mekhilef S, Mokhlis H, Kermadi M, Alshammari O. Performance analysis of hybrid off-grid renewable energy systems for sustainable rural electrification. Energy Convers Manage: X 2024;24:100780. https://doi.org/10.1016/j.ecmx.2024.100780.
[77] Koholé YW, Wankouo Ngouleu CA, Fohagui FCV, Tchuen G. Optimization and comparative analysis of hybrid renewable energy systems for sustainable and clean energy production in rural Cameroon considering the loss of power supply probability concept. Energy Convers Manage: X 2025;25:100829. https://doi.org/10.1016/j.ecmx.2024.100829.
[78] Lau KY, Tan CW, Yatim AHM. Photovoltaic systems for Malaysian islands: effects of interest rates, diesel prices and load sizes. Energy 2015;83:204–16. https://doi.org/10.1016/j.energy.2015.02.015.
[79] Adaramola MS, Paul SS, Oyewola OM. Assessment of decentralized hybrid PV solar-diesel power system for applications in Northern part of Nigeria. Energy Sustain Develop 2014;19:72–82. https://doi.org/10.1016/j.esd.2013.12.007.
[80] Ba-swaimi S, Verayiah R, Ramachandaramurthy VK, ALAhmad AK, Abu-Rayash A. Development and techno-economic assessment of an optimized and integrated solar/wind energy system for remote health applications. Energy Convers Manage: X 2025;26:100985. https://doi.org/10.1016/j.ecmx.2025.100985.
[81] Fathi Nassar Y, Yassin AS. Assessment of solar energy potential in Gaza Strip-Palestine. Sustain Energy Technol Assessments 2019;31:318–28. https://doi.org/10.1016/j.seta.2018.12.010.
[82] Kácsor E, Mezősi A, Szabó L. Integrating solar plants into the European power grid – what is the optimal capacity combination of PV and battery storage? Energy Convers Manage: X 2025;26:101029. https://doi.org/10.1016/j.ecmx.2025.101029.
[83] Rezzouk H, Mellit A. Feasibility study and sensitivity analysis of a stand-alone photovoltaic–diesel–battery hybrid energy system in the north of Algeria. Renew Sustain Energy Rev 2015;43:1134–50. https://doi.org/10.1016/j.rser.2014.11.103.
[84] Shabani M, Yan J. Optimization and evaluation of operational and economic performance of grid-connected battery storage at different stages of battery health. Energy Convers Manage: X 2025;27:101113. https://doi.org/10.1016/j.ecmx.2025.101113.
[85] Wang L, Qiu J, Wang X, Chen L, Cao G, Wang J, et al. Insights for understanding multiscale degradation of LiFePO4 cathodes. Escience 2022;2:125–37. https://doi.org/10.1016/j.esci.2022.03.006.
[86] Megantoro P, Halim SA, Mohamed Kamari NA, Awalin LJ, Mohamed R, Rosli HM. An enhanced multi-objective reactive power dispatch for hybrid Wind-Solar power system using Archimedes optimization algorithm. Int J Electr Power Energy Syst 2025;168:110676. https://doi.org/10.1016/j.ijepes.2025.110676.